1H NMR spectroscopy of strongly J-coupled alcohols acquired at 50 mT (2 MHz) using a Carr-Purcell-Meiboom-Gill echo technique

Ronen, I.; Webb, A.G.

Conference paper

Itamar Ronen* and Andrew G. Webb

^{1}H NMR spectroscopy of strongly J-coupled alcohols acquired at 50 mT (2 MHz) using a Carr–Purcell–Meiboom–Gill echo technique

https://doi.org/10.1515/pac-2023-0102

Abstract: We have investigated an approach for obtaining ^{1}H NMR spectra of different alcohols on a large-bore (27 cm diameter), B_0 = 0.05 T (f_0 = 2 MHz) portable MRI scanner. We used a Carr–Purcell–Meiboom–Gill (CPMG) sequence to acquire multiecho data from solutions of different alcohols, focusing on ethanol, a molecule of relevance to many applications in the food and beverage industry. Our results show that the Fourier transformed J-spectra at different echo spacings fit well with simulations of the evolution of the echo train signal with excellent signal to noise ratio (SNR) for concentrations of ~10 % within a few minutes. Spectra were also obtained from intact bottles of whiskey and wine. Finally, we show that different alcohols with similar chemical structures can be differentiated using this approach.

Keywords: Alcohols; food and beverage analysis; Italian-French NMR conference; J spectroscopy; Low field NMR.

Introduction

Low-field NMR finds many applications in the food and drink industry [1]. Broadly speaking, NMR systems used for these applications are: (i) standard high resolution systems which can perform spectroscopic studies on small samples, (ii) imaging systems (primarily designed for pre-clinical animal studies) which can perform spectroscopy on larger samples, or (iii) low-field systems which can be used for relaxometric measurements. High resolution NMR spectroscopy gives the most detailed chemical information about the sample, but is limited by the high cost of such equipment [2, 3] and the small sample sizes that can be investigated. For example, high resolution NMR has been used to estimate alcohol (as well as other molecules) concentrations in beverages [4]. Smaller and less expensive systems based on permanent magnets have also been developed for spectroscopic studies. For example, the Magritek Spinsolve (https://magritek.com/products/benchtop-nmr-spectrometer-spinsolve/spinsolve-60/) operates at 60 MHz and can achieve very low proton linewidths (Spinsolve 60 Ultra: <0.2 Hz (50 %)/<7 Hz (0.55 %)/<14 Hz (0.11 %)). For example, this system has been used to obtain differentiate between a large number of different fentanyl analogues [5]. This system has also been used for quantitative analysis, based on high resolution spectroscopy, of several beverages [6]. Ethanol content of samples has also been assessed at 45 MHz [7]. However, these measurements are also limited to small sample volumes, typically a few mL or less. There have been several studies of intact bottles of wine, including those performed using a superconducting 2 T magnet [8] or 4.7 T superconducting magnet [9]: these systems have the advantage of being able to study large (intact) samples, but the disadvantage of requiring large and very expensive setups. Relaxometric techniques [10] can be used, for example, to measure the ratio of water and lipid in food samples. Single-sided magnets allow

Article note: A collection of invited papers based on presentations at the Italian-French International Conference on Magnetic Resonance, Milan, Italy, 27–30 September 2022.

***Corresponding author: Itamar Ronen**, Clinical Imaging Sciences Centre, Brighton and Sussex Medical School, University of Sussex, Falmer BN1 9RR, UK, e-mail: i.ronen@bsms.ac.uk

Andrew G. Webb, C. J. Gorter MRI Center, Department of Radiology, Leiden University Medical Center, Leiden, The Netherlands

increased flexibility in the samples that can be studied [11, 12]. These systems are typically based on permanent magnet assemblies, and do not require high B_0 homogeneity to make the measurements. However, the homogeneity of such permanent magnet systems is much too low to be able to acquire high resolution proton spectra. From the above summary, one setup which is currently missing is one which allows the possibility to perform spectroscopic studies on large samples using an inexpensive NMR system, i.e. one based on permanent magnets rather than superconducting, technology.

In this work we extend a previous investigation [13] of the use of scalar coupling (J)-evolution during Carr–Purcell–Meiboom–Gill (CPMG) sequences to acquisition of J-spectra of coupled spins using a 50 mT, relatively inhomogeneous B_0 field. In conventional high field NMR the difference in resonance frequencies due to chemical shift (which is proportional to the magnetic field) between various protons in a small molecule is typically much larger than the scalar coupling constant (which is field independent and typically lies in the range 1–7 Hz). This means that the fine structure in the NMR spectrum is relatively easily analyzed with the multiplet structures of distinct chemical shifts providing information about the number of protons on each carbon atom, and therefore the chemical structure. At much lower fields the chemical shift differences and scalar coupling are on the same order as each other, which means that the spectra become much more complicated and difficult to predict analytically. A very high B_0 homogeneity is also necessary to separate the very small differences in frequency between the peaks. Using CPMG-based J-spectroscopy [14], in contrast, the signal along the echo train evolves according to the underlying scalar couplings [15, 16]. One particularly attractive property of the evolution of the echo series along the echo time dimension is that its decay rate is dictated by T_2 rather than T_2^*, and therefore the B_0 homogeneity is not critical if the J-coupling evolves sufficiently throughout the echo train. Here we study ethanol, a molecule of interest to the food and beverage industry, and determine the parameters for optimal spectroscopic detection. We simulated the spectra of this more complex A_3B_2 system (where the A refers to the methyl group and B to the methylene) and compared simulation with experiment. We also investigated whether similar alcohols, such as 2-propanol and 1,2-dipropanediol, would give sufficiently different J-coupled spectra to be able to differentiate the molecules.

Experimental

Materials

Samples of 10 % ethanol, 2-propanol and 1,2-dipropanediol in D_2O (all from Sigma Aldrich, St. Louis MO, USA) and H_2O were prepared. About 30 cc of each solution were injected into table-tennis balls (diameter 30 mm), and the hole in the injection site was sealed with hot glue. Bottles of wine (~14 % alcohol) and whiskey (~40 % alcohol) were used intact: the dimensions of both bottles were ~30 cm in height and ~8 cm in diameter. Table 1 shows the chemical structure and nomenclature for the hydrogen nuclei in the three different molecules.

Table 1: Molecular structure, chemical formulae and NMR characteristics of alcohols investigated in this work.

	1,2-propanediol	2-propanol	ethanol
Molecular structure	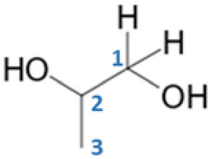	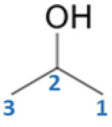	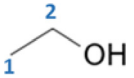
Chemical formula	CH_3–CHOH–CH_2OH	CH_3–CHOH–CH_3	CH_3–CH_2OH
Spin system at B_0 = 55 mT (excluding hydroxyl protons)	A_3BC_2	A_6B	A_3B_2
Chemical shifts (ppm) and coupling constants (Hz)	δ_{H1} = 3.54, J_{H1-H2} = 4.0 δ_{H2} = 3.89, J_{H2-H3} = 6.5 δ_{H3} = 1.15	$\delta_{H1,H3}$ = 1.20, $J_{H2-H1,H3}$ = 6.1 δ_{H2} = 4.01	δ_{H1} = 1.23, J_{H1-H2} = 7.0 δ_{H2} = 3.7

Instrumentation

All experiments were performed on a custom-built MRI scanner operating at B_0 = 0.05 T with a 27 cm diameter bore, described in detail previously [17]. The B_0 field is generated using a large number of permanent magnets arranged in a cylindrical dipolar Halbach array configuration and is directed across the bore of the scanner. Three linear gradient coils were used to perform first order shimming over the sample. A 3.5 cm diameter, 7 cm long solenoidal coil wound with copper wire was used as the RF transceiver coil for the table-tennis ball samples. A larger solenoid (12 cm diameter, 20 cm length) was used for the whole bottle experiments. The measured linewidth for the table tennis ball samples was ~50 Hz and for the wine bottle ~150 Hz. A Magritek Kea2 spectrometer (Aachen, Germany) was used to generate the low power RF pulses which were subsequently amplified by a custom built RF amplifier. The spectrometer features a built-in transmit/receive switch used to route the amplified signal to the RF coil.

Simulations

All simulations were performed with in-house Matlab® (Mathworks, Natick MA, USA) programmes using the density matrix formalism, assuming a Hamiltonian that consisted of Zeeman and scalar coupling terms. RF pulses were assumed to be infinitely narrow pulses with flip angles of 90° and 180° [18] (for the Matlab-based simulation platform see [19]). Values for the chemical shifts and the scalar coupling values for ethanol, 2-propanol and 1,2-propanediol were taken from the Spectral Database for Organic Compounds, SDBS (AIST, Japan, https://sdbs.db.aist.go.jp/sdbs/cgi-bin/cre_index.cgi). To provide a simulated line width matching that of the experimentally acquired J-spectra, simulated echo trains were multiplied with an exponential decay function that approximated the T_2 of the sample, prior to Fourier transform.

Pulse sequences

The CPMG sequence was modified to allow the first echo time ($2\tau_1$) to be set independently of subsequent echo times (2τ). This minimizes phase accrual between the excitation pulse and the first echo. A pulse duration of 100 μs was used for 90° and 180° pulses in all experiments. Typical parameters for the CPMG acquisition were: time-of-repetition (TR) between signal averages =20 s, number of averages 8, spectral bandwidth 5 kHz, number of complex data points 64, producing an acquisition time of 12.8 ms symmetrically positioned around the centre of the echo, $2\tau_1$ = 16 ms, and different 2τ values in the range of 50–125 ms were investigated. The number of echoes was either 128 or 256, with fewer echoes for the longer inter-pulse delays.

Data processing

Each data set comprised an $N \times M$ matrix, where N is the number of points acquired at each echo and M is the number of echoes. These were read into Matlab® and analysed with in-house routines. Data from both sides of the echo peak were combined according to $S = S^+ + (S^-)^*$ where S^+ represents data points for $N/2 + 1 \le n \le N$, and S^- where $1 \le n \le N/2$ with the data point order reversed: * represents the complex conjugate. The resulting "symmetrized" data was Fourier transformed along the time domain to yield M complex spectra. The echo maxima were used as a single complex value for each echo. The series of M echo maxima was zero-filled to $2*M$ and Fourier transformed to yield the J-spectrum. Removal of the central peak, containing the contribution of uncoupled spins and unresolved resonances was performed based on a Hankel singular value decomposition method (HSVD) [13].

Results and discussion

Figure 1 shows a typical spectrum (blue dotted line) obtained from an FID collected from the pure ethanol phantom: the linewidth is clearly non-Lorentzian, reflecting primarily the B_0 inhomogeneities with a small contribution from the underlying spectral structure. Also shown on the same frequency scale is the simulated spectrum of ethanol assuming a linewidth of 0.02 Hz: the spectrum represents a strongly coupled A_3B_2 system, complicating the spectrum compared to that acquired at higher fields [20], and also showing weak outer spectral lines.

Figure 2 shows simulated and experimental data acquired with the CPMG sequence from a phantom that contained 10 % ethanol in D_2O, as a function of the inter-pulse time. Good agreement can be seen between the multi-line simulations and experimental data, which show very different spectral patterns depending upon the choice of inter-pulse time.

In "real-life" samples there is a large contribution from the non-coupled water signal, which results in a large zero-frequency peak in the J-spectrum. In addition, as can be seen in the spectra in panel b of Fig. 2, a significant portion of the J spectrum results in peaks which are also very close to zero frequency. Figure 3 shows spectra acquired from the whiskey and wine samples, using intact bottles placed inside the larger solenoid coil. Again, the spectra show the expected peak distributions based on simulations shown previously.

The final experiments were performed to determine whether there were resolvable differences in spectral patterns from three different alcohols, ethanol, 2-propanol and 1,2-dipropanediol. Figure 4 shows experimental data from samples of 10 % of the different alcohols in D_2O.

Discussion and conclusion

In this work we have demonstrated the possibility of obtaining unique spectral information on different alcohols using a large bore 50 mT scanner with relatively inhomogeneous magnetic field. Using this type of system directly obtaining 1D spectra from the FID in a pulse-acquire experiment is not possible, as shown in Fig. 1. However, J-spectroscopy, or the Fourier transform of the series of echoes acquired with a CPMG sequence, retains the information on spin-spin couplings, and well-resolved J-spectra can be obtained. As shown by the simulations and experiments the spin systems are all strongly coupled, and under these conditions the relationships between the chemical shifts, scalar coupling constants and the π–π inter-pulse delays all contribute to the resulting pattern of the resulting J-spectrum for each molecule. Analytical solutions for the standard spectra of some strongly coupled systems exist, but for more complex cases, including the A_3B_2 system of ethanol, spectral simulation is required. We note that another technique, termed spin-lock induced crossing (SLIC), can also be used to acquire spectra at even lower fields, in this case 6 mT [20].

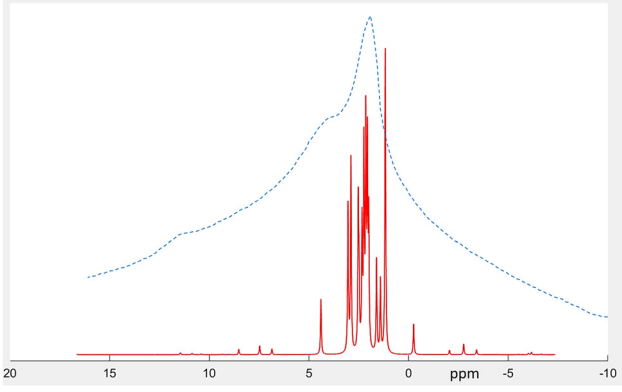

Fig. 1: (Red line) simulations of the NMR spectrum of ethanol at 0.05 T assuming a linewidth of 0.02 Hz. (Blue line) overlay of the experimental proton spectrum acquired after shimming a spherical sample (diameter 30 mm) of pure ethanol in the 0.05 T Halbach array.

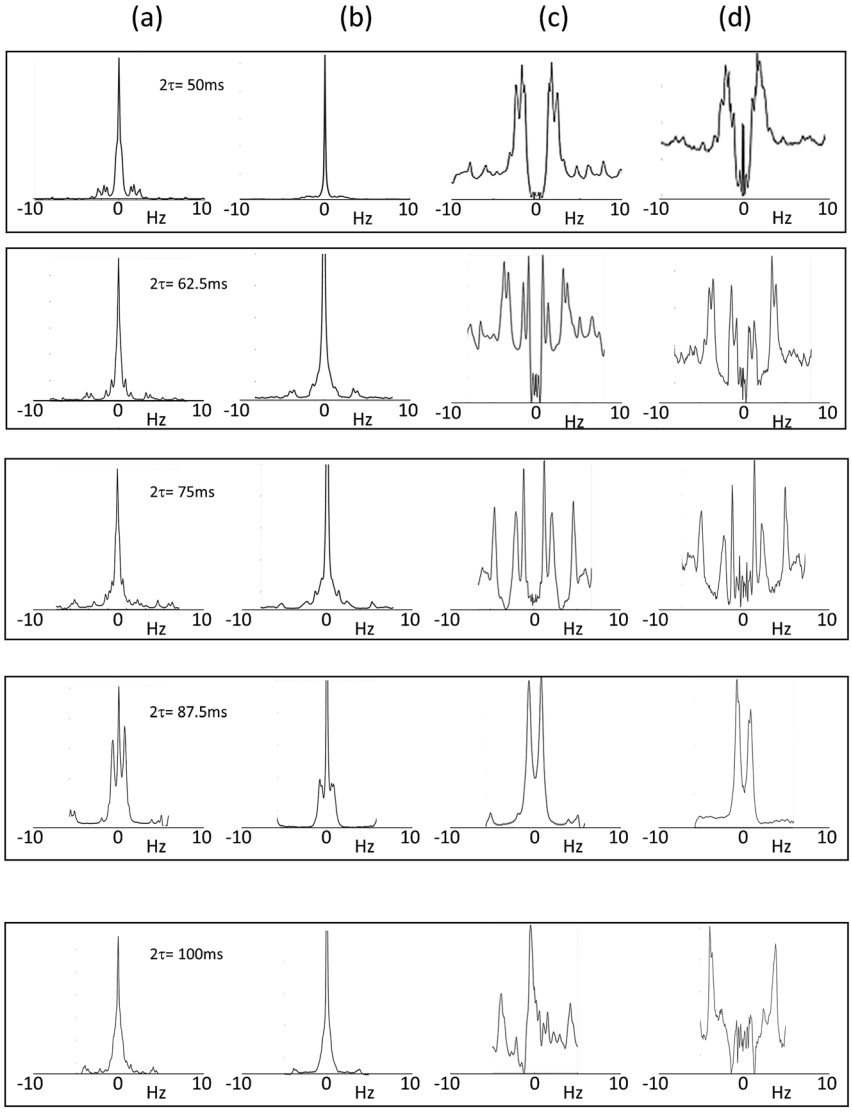

Fig. 2: Simulations and experimental data for 10 % ethanol in D_2O acquired using different inter-pulse delays. (a) Simulated spectra, (b) experimental spectra, (c) simulated spectra after notch filtering to remove the singlet peak at zero frequency, and (d) experimental spectra after notch filtering.

A significant challenge for J-spectroscopy is the removal of the peak around zero frequency, consisting of the contributions from water protons and all other singlets, as well as from unresolved low frequency peaks in the J spectrum. One possible approach is to notch the peak in the post-processing stage, as we demonstrated here with the use of HSVD. Another approach, which we showed in a previous publication [13], is to acquire an additional J-spectrum in which the modulation induced by the scalar coupling is removed with the use of the J-refocused CPMG sequence [21, 22]. This latter approach is equivalent to spectral editing in standard spectroscopy. Removal of the central peak in this way offers some advantages, such as retaining some sensitivity to the unresolved J-coupled peaks in the vicinity of the peak at 0 Hz frequency. The main disadvantage is the penalty in SNR due to the addition of noise in the subtraction process.

We showed in our previous publication that quantification using a simple HSVD approach for peak fitting is possible, and allows also the estimation of the error in quantification (Cramer Rao lower bounds). For reliable across-sample quantification of a set of known molecules, such as ethanol and other alcohols in the present case, a more reliable approach is required. One possible approach is the one implemented in standard spectroscopic quantification, that of using a set of known spectral patterns for each molecule as priors, and subsequently solving the least mean square linear system for the concentrations of each molecule [23]. This approach is robust if the linear dependence between the various components of the “basis set” (i.e. the spectral similarity) is low. The

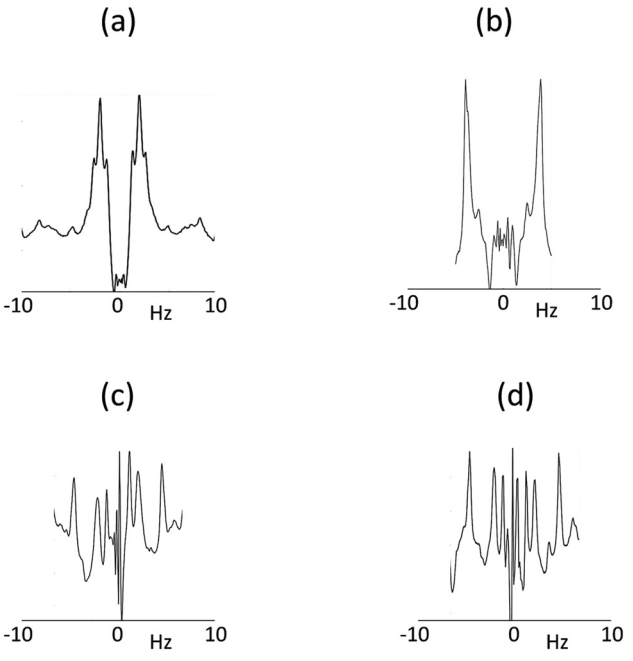

Fig. 3: Spectra obtained from a whiskey sample (a–c) and wine sample (d). Inter-pulse delays were: (a) 50 ms, (b) 100 ms, (c) and (d) 75 ms. Notch filtering was applied for all spectra.

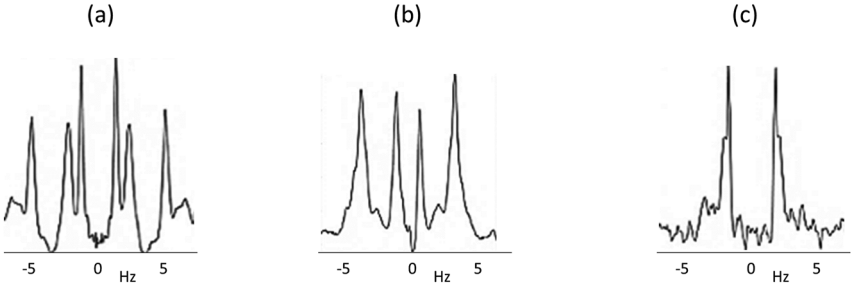

Fig. 4: Spectra of (a) 10 % ethanol in D_2O, (b) 10 % 2-propanol in D_2O and (c) 10 % 1,2-dipropanediol in D_2O, all acquired using a $2\tau = 75$ ms interpulse delay. Notch filtering was applied for all spectra.

spectral content of J-spectra is uniquely defined by the spin system that characterizes the molecule of interest, and by a single experimental variable – the inter-pulse delay in the CPMG sequence. The optimal inter-pulse delay for quantification of a specific molecule is a trade-off between signal to noise ratio (SNR) and spectral separability of the peaks, and will depend on several considerations. The simplest consideration is that shorter inter-pulse delays result in better sampling of the echo train and thus in overall higher SNR for the entire J-spectrum. More complicated considerations arise from the characteristics of the spectral patterns expected for specific molecules. For the molecules and the field strength in our experiments, the scalar coupling constants between protons, J, are equal or larger than δ, the differences in resonance frequencies between coupled protons. For such strongly coupled systems, the evolution of the scalar coupling along the echo train strongly depends on the inter-pulse delay: the longer the delay is, the higher are the frequencies in the echo train and in the resulting J-spectrum [16, 24]. This would indicate that spectral separability is improved with longer inter-pulse delays. This is however compounded by the fact that the inter-pulse delay is equal to the time between subsequent echoes and thus dictates the spectral width (SW) of the J-spectrum such that SW = 1/(inter-pulse delay). Thus, at longer inter-pulse delays the higher frequency components of the J-spectrum can become undersampled and are then folded into the actual spectral bandwidth [25]. Finer details of the J-spectrum are also affected by the choice of inter-pulse delay, of which the most relevant is the distribution of peak amplitudes across the spectrum. In the simple case of an AB system (two spin system with $J \approx \delta$), an analytical solution for the spectral content of the CPMG echo train has been provided [24]. Figure 5(a) shows simulated J-spectra for an AB system with $J = 7$ Hz, $\delta = 6.45$ Hz (3 ppm at $B_0 = 50$ mT) and three different inter-pulse delays. Besides the overall higher intensity at shorter inter-pulse

delays, it can be seen that for inter-pulse delay of 25 ms, the amplitude of the inner peaks (lower frequencies) is significantly higher than that of the outer, high frequency peaks. For the longer inter-pulse delays of 50 and 75 ms, the amplitude difference between the two pairs of peaks gradually decreases. Figure 5b shows simulated J-spectra of isopropanol (2-propanol) at three inter-pulse delays. While the overall SNR of the J-spectrum at the shortest inter-pulse delay is the highest (central peak is truncated at less than half its maximum), most of the spectral content coalesces with the central spectral line (zero frequency), making it practically indistinguishable from the spectral contribution of non-coupled protons that may be present, for example water protons or the labile OH protons. Both longer delays show well separated side peaks, and for this particular case it appears that an inter-pulse delay of 50 ms is close to an optimum.

The major advantage of this approach is that it allows large samples, i.e. intact bottles, to be studied, unlike the case for high resolution NMR where the limited bore-size requires the removal of small aliquots. Although one could potentially use a horizontal-bore preclinical imaging system, the cost, maintenance and siting requirements of such a system are orders of magnitude larger than those required for the permanent magnet based system used in this study. Having pre-simulated the spectrum of the molecule of interest, in this case ethanol, the processing of each spectrum can easily be performed in a manner of seconds using the algorithms outlined in this paper (the algorithms will be made available upon request to the first author).

Future work will focus on the attainable data quality using intact bottles of different beverages. The major challenges are anticipated to be the greater B_0 and RF transmit field (B_1) inhomogeneities due to the much larger sample. Our previous work showed that the spectral patterns are quite sensitive to the B_1 distribution, and so this effect must be taken into account. The B_1 issue can be addressed by using separate transmit and receive coils, either electrically or geometrically decoupled from one another. A large transmit RF coil can be used to produce a homogeneous B_1 field, whereas a smaller tight-fitting receive RF coil can be used for high SNR. A smaller RF receive coil can also be used to reduce the effective volume over which signal is received, which reduces the effective B_0 inhomogeneity. Since the signal from the CPMG sequence is dictated by T_2 rather than T_2* effects, provided that the B_0 is homogeneous enough that off-resonance effects from RF pulses do not play a significant role, we anticipate that the B_0 effect will not be a major factor. There is also the possibility to use multiple receive coils, as is commonly done in MRI studies. However, the SNR advantage is likely to be small since overall system noise is coil dominated in this frequency range using typically very low loss samples.

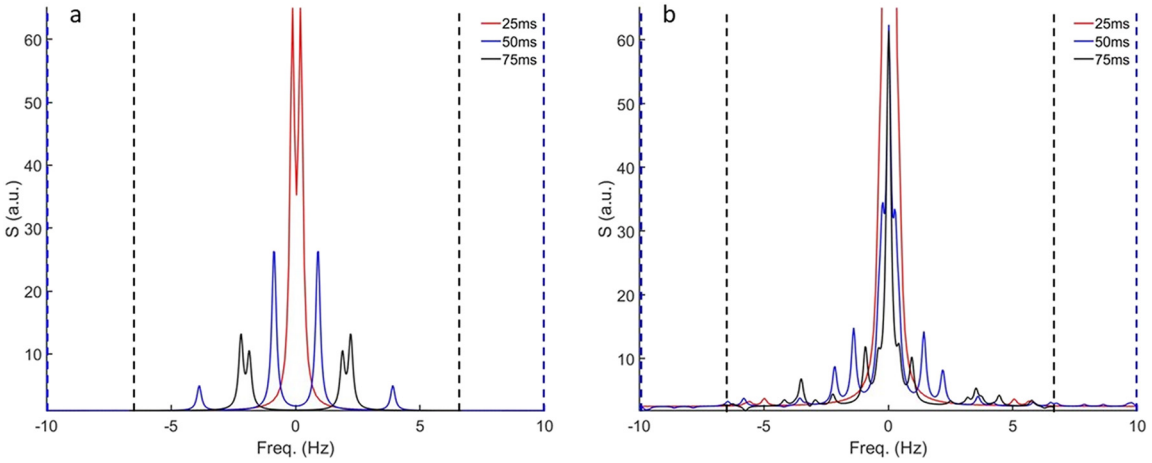

Fig. 5: Simulated spectra two spin systems at B_0 = 50 mT: (a) hypothetical AB system with J = 7 Hz and δ = 3 ppm = 6.45 Hz and (b) isopropanol (A_6B system, J = 6.1 Hz and δ = 2.8 ppm = 6.02 Hz). In both cases the T_2 was set at 1500 ms. Dashed lines mark the spectral width for the corresponding inter-pulse delay (the frequency range in both panels was set at 15 Hz for clearer visualization of the spectral patterns). The overall signal for both spin systems is highest at the shortest inter-pulse delay (25 ms). Stronger side peaks are visible for both spin systems at the longer delay values. The choice of inter-pulse delay for quantification purposes will depend on a combination of both factors – overall SNR and spectral separability.

Acknowledgments: We thank Dr. Pierre-Gilles Henry from the Center for Magnetic Resonance Research at the University of Minnesota for providing us with the simulation platform we used in this work.
Research funding: This project has received funding from Horizon 2020 ERC Advanced PASMAR 101021218 and the Dutch Science Foundation Open Technology Grant number 18981.

References

[1] A. P. Sobolev, C. Ingallina, M. Spano, G. Di Matteo, L. Mannina. *Molecules* **27**, 7906 (2022), https://doi.org/10.3390/molecules27227906.
[2] P. A. Solovyev, C. Fauhl-Hassek, J. Riedl, S. Esslinger, L. Bontempo, F. Camin. *Compr. Rev. Food Sci. Food Saf.* **20**, 2040 (2021), https://doi.org/10.1111/1541-4337.12700.
[3] E. Hatzakis. *Compr. Rev. Food Sci. Food Saf.* **18**, 189 (2019), https://doi.org/10.1111/1541-4337.12408.
[4] E. Lopez-Rituerto, S. Cabredo, M. Lopez, A. Avenoza, J. H. Busto, J. M. Peregrina. *J. Agric. Food Chem.* **57**, 2112 (2009), https://doi.org/10.1021/jf803245r.
[5] J. Duffy, A. Urbas, M. Niemitz, K. Lippa, I. Marginean. *Anal. Chim. Acta* **1049**, 161 (2019), https://doi.org/10.1016/j.aca.2018.12.014.
[6] Y. Matviychuk, S. Haycock, T. Rutan, D. J. Holland. *Anal. Chim. Acta* **1182**, 338944 (2021), https://doi.org/10.1016/j.aca.2021.338944.
[7] M. F. Isaac-Lam. *Int. J. Spectrosc.* **2016**, Article 2526946 (2016), https://doi.org/10.1155/2016/2526946.
[8] A. J. Weekley, P. Bruins, M. Sisto, M. P. Augustine. *J. Magn. Reson*. **161**, 91 (2003), https://doi.org/10.1016/s1090-7807(02)00177-5.
[9] D. N. Sobieski, G. Mulvihill, J. S. Broz, M. P. Augustine. *Solid State Nucl. Magn. Reson.* **29**, 191 (2006), https://doi.org/10.1016/j.ssnmr.2005.08.014.
[10] E. Kirtil, S. Cikrikci, M. J. McCarthy, M. H. Oztop. *Curr. Opin. Food Sci.* **17**, 9 (2017), https://doi.org/10.1016/j.cofs.2017.07.005.
[11] A. Guthausen, G. Guthausen, A. Kamlowski, H. Todt, W. Burk, D. Schmalbein. *J. Am. Oil Chem. Soc*. **81**, 727 (2004), https://doi.org/10.1007/s11746-004-0969-5.
[12] D. Capitani, A. P. Sobolev, V. Di Tullio, L. Mannina, N. Proietti. *Chem. Biol. Technol. Agric.* **4**, 17 (2017), https://doi.org/10.1186/s40538-017-0100-1.
[13] I. Ronen, T. O'Reilly, M. Froeling, A. G. Webb. *J. Magn. Reson*. **320**, 106834 (2020), https://doi.org/10.1016/j.jmr.2020.106834.
[14] S. Meiboom, D. Gill. *Rev. Sci. Instrum*. **29**, 688 (1958), https://doi.org/10.1063/1.1716296.
[15] R. L. Vold, R. R. Vold. *Prog. Nucl. Magn. Reson. Spectrosc.* **12**, 79 (1978), https://doi.org/10.1016/0079-6565(78)80004-1.
[16] A. J Allerhan. *Chem. Phys*. **44**, 1 (1966).
[17] T. O'Reilly, W. M. Teeuwisse, A. G. Webb. *J. Magn. Reson*. **307**, 106578 (2019), https://doi.org/10.1016/j.jmr.2019.106578.
[18] R. V. Mulkern, J. L. Bowers. *Magn. Reson. Med.* **30**, 518 (1993), https://doi.org/10.1002/mrm.1910300418.
[19] P. G. Henry, M. Marjanska, J. D. Walls, J. Valette, R. Gruetter, K. Ugurbil. *Magn. Reson. Med.* **55**, 250 (2006), https://doi.org/10.1002/mrm.20764.
[20] S. J. DeVience, M. Greer, S. Mandal, M. S. Rosen. *Chemphyschem* **22**, 2128 (2021), https://doi.org/10.1002/cphc.202100162.
[21] K. Takegoshi, K. Ogura, K. Hikichi. *J. Magn. Reson.* **84**, 611 (1989), https://doi.org/10.1016/0022-2364(89)90127-3.
[22] P. C. M. Vanzijl, C. T. W. Moonen, M. Vonkienlin. *J. Magn. Reson.* **89**, 28 (1990), https://doi.org/10.1016/0022-2364(90)90159-7.
[23] S. W. Provencher. *Magn. Reson. Med.* **30**, 672 (1993), https://doi.org/10.1002/mrm.1910300604.
[24] E. J. Wells, H. S. Gutowsky. *J. Chem. Phys*. **43**, 3414 (1965), https://doi.org/10.1063/1.1726421.
[25] A. Bax, A. F. Mehlkopf, J. Smidt. *J. Magn. Reson*. **40**, 213 (1980), https://doi.org/10.1016/0022-2364(80)90242-5.